/N-61
37981
P. 40

NASA Technical Memorandum

NASA TM - 103550

EMPIRICAL PREDICTIONS OF HYPERVELOCITY IMPACT DAMAGE TO THE SPACE STATION

By W.K. Rule and K.B. Hayashida

Structures and Dynamics Laboratory
Science and Engineering Directorate

July 1991

(NASA-TM-103550) EMPIRICAL PREDICTIONS OF HYPERVELOCITY IMPACT DAMAGE TO THE SPACE STATION (NASA) 40 p CSCL 09B
N91-30751
Unclas
G3/61 0037981

National Aeronautics and Space Administration
George C. Marshall Space Flight Center

MSFC - Form 3190 (Rev. May 1983)

REPORT DOCUMENTATION PAGE

Form Approved
OMB No. 0704-0188

1. AGENCY USE ONLY *(Leave blank)*

2. REPORT DATE
July 1991

3. REPORT TYPE AND DATES COVERED
Technical Memorandum

4. TITLE AND SUBTITLE
Empirical Predictions of Hypervelocity Impact Damage to the Space Station

5. FUNDING NUMBERS

6. AUTHOR(S)
W.K. Rule* and K.B. Hayashida

7. PERFORMING ORGANIZATION NAME(S) AND ADDRESS(ES)
George C. Marshall Space Flight Center
Marshall Space Flight Center, Alabama 35812

8. PERFORMING ORGANIZATION REPORT NUMBER

9. SPONSORING/MONITORING AGENCY NAME(S) AND ADDRESS(ES)
National Aeronautics and Space Administration
Washington, DC 20546

10. SPONSORING/MONITORING AGENCY REPORT NUMBER
NASA TM-103550

11. SUPPLEMENTARY NOTES
Prepared by Structures and Dynamics Laboratory, Science and Engineering Directorate.
*University of Alabama, Tuscaloosa, Alabama.

12a. DISTRIBUTION/AVAILABILITY STATEMENT
Unclassified-Unlimited

12b. DISTRIBUTION CODE

13. ABSTRACT *(Maximum 200 words)*

This report describes a family of user-friendly, DOS PC based, Microsoft BASIC programs written to provide spacecraft designers with empirical predictions of space debris damage to orbiting spacecraft. The spacecraft wall configuration is assumed to consist of multilayer insulation (MLI) placed between a Whipple style bumper and the pressure wall. Predictions are based on data sets of experimental results obtained from simulating debris impacts on spacecraft using light gas guns on Earth. A module of the program facilitates the creation of the data base of experimental results that are used by the damage prediction modules of the code. The user has the choice of three different prediction modules to predict damage to the bumper, the MLI, and the pressure wall. One prediction module is based on fitting low order polynomials through subsets of the experimental data. Another prediction module fits functions based on nondimensional parameters through the data. The last prediction technique is a unique approach that is based on weighting the experimental data according to the distance from the design point.

14. SUBJECT TERMS
Hypervelocity Impact, Orbital Debris, Multilayer Insulation, Empirical Prediction, Space Station

15. NUMBER OF PAGES
40

16. PRICE CODE
NTIS

17. SECURITY CLASSIFICATION OF REPORT	18. SECURITY CLASSIFICATION OF THIS PAGE	19. SECURITY CLASSIFICATION OF ABSTRACT	20. LIMITATION OF ABSTRACT
Unclassified	Unclassified		Unlimited

NSN 7540-01-280-5500

Standard Form 298 (Rev. 2-89)

TABLE OF CONTENTS

LIST OF ILLUSTRATIONS

LIST OF TABLES

LIST OF SYMBOLS

b	y intercept of regression equation
C_i	coefficients in polynomial or nondimensional prediction functions
D_i	value of dependent variable (impact damage) at the ith data point
D_{MAX}	maximum diameter of the bumper hole
D_{MIN}	minimum diameter of the bumper hole
D_{MLI}	average diameter of the hole in the MLI
D_p	diameter of projectile
D_{pw}	average diameter of the pressure wall hole
D_s	bumper stand-off distance
D	estimated value of dependent variable (impact damage) at an interpolation or prediction point
E	elastic modulus of the bumper plate material
m	slope of regression equation
M	number of data points in data base or number of material properties in each record of the materials data file
N	number of independent variables (impact parameters)
rn#	random number used to generate test function
R^2	coefficient of determination
R_i	distance from ith data point to interpolation or prediction point
S	length of influence of a data point
T_b	bumper thickness
T_{pw}	pressure wall thickness
V	projectile velocity
V_s	speed of sound in the bumper material = $\sqrt{E/\rho}$
x	measured value in linear regression equation

$x_{j,i}$	jth coordinate (independent variable) of ith data point
$x_{j,\mathrm{INT}}$	jth coordinate (independent variable) of interpolation or prediction point
$\Delta x_{j,i}$	$x_{j,i}-x_{j,\mathrm{INT}}$
y	predicted value in linear regression equation
ϕ	impact angle
ρ	mass density of the bumper plate material
θ	weighting factor of a data point

TECHNICAL MEMORANDUM

EMPIRICAL PREDICTIONS OF HYPERVELOCITY IMPACT DAMAGE TO THE SPACE STATION

I. INTRODUCTION

There are many engineering applications where predictions of the behavior of a physical system must be made based on a data base of experimental results. In these instances, either the phenomenon is too complicated to treat analytically or numerically, or the funding, expertise, or time required to do so is not available. Empirical approaches of this nature have always played a fundamental role in engineering design.

The purpose of the project described in this report was to develop a DOS microcomputer-based computer program to empirically predict hypervelocity impact damage to the Space Station *Freedom* from space debris. The main goal was to predict damage to the multilayer insulation (MLI). However, to extend the usefulness of the program, damage to other components of the space station wall can be predicted as well. The program is intended to be an easy-to-use design tool for trade studies on debris protection strategies for the Space Station *Freedom*. The predictions are made based on a data base of experimental results.

Marshall Space Flight Center (MSFC) has a light gas gun that can launch 2.5- to 12.7-mm projectiles at speeds of 2 to 8 km/s.[1] Work is currently in progress at MSFC to qualify the orbital debris protection system under development by Boeing Aerospace and Electronics for Space Station *Freedom*. A schematic of the protection system is shown in figure 1. It is based on the classical sacrificial bumper approach first suggested by Whipple.[2] The purpose of the bumper is to breakup or ideally vaporize the projectile (space debris or micrometeoroids) so that the pressurized spacecraft behind the bumper is impacted with a cloud of fine particles rather than a single large particle.

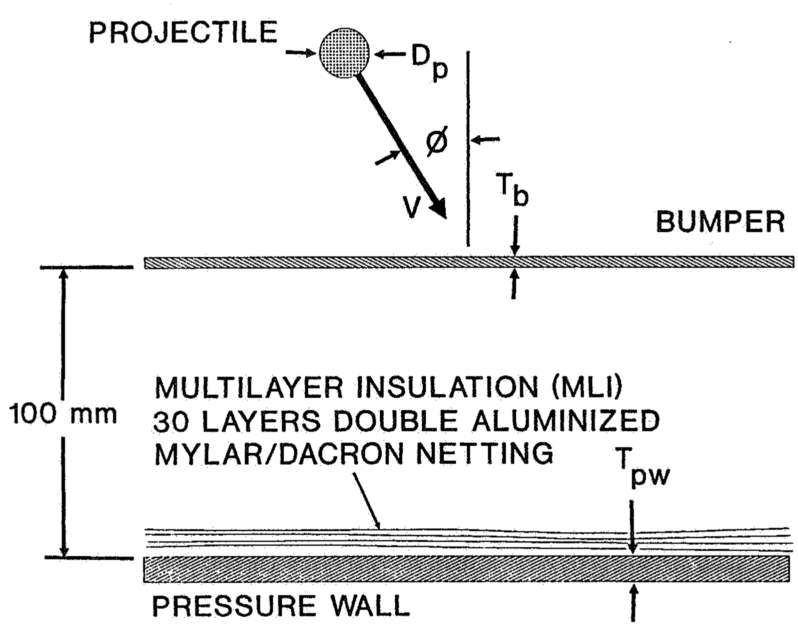

Figure 1. Schematic drawing of impact specimen.

The parameters associated with the impact data are illustrated in figure 1. The projectiles were initially spherical and were typically constructed of 1100-0 aluminum. The bumper and the pressure walls were usually made from 6061-T6 and 2219-T87 aluminum, respectively. Some tests have been run with different materials.

There are seven computer programs that were developed for this project. Details of how to use the family of programs are provided in section II. A main program called MLIBLAST serves as a shell to run the other six programs. Programs called DATABASE, DBASEDEL, and DBASEOUT are provided to assist the user in creating and maintaining data base files of experimental results.

The remaining three programs provide predictions of impact damage to the bumper, the MLI, and the pressure wall plate. Program INVRMETH uses a unique prediction technique, called the inverse *R* method, that was developed for the purposes of this project. The theoretical basis of this method is described in section III.

As described in section IV, program POLYMETH makes predictions by fitting simple polynomials through a subset of data points. A more sophisticated form of polynomial prediction technique using the isoparametric formulation of the finite element method (FEM) as a basis was also attempted during the course of this project. This FEM-based software was found to be somewhat unreliable for making predictions from the impact data that is currently available and so it was not included with this software. The interested reader can consult reference 3 for a discussion of this method.

The last prediction program, NONDIMEN, makes predictions based on nondimensionalized functions that were developed by others and extended by the authors for application here. These functions are described in section V. The relative accuracies of these three prediction schemes are compared using an actual impact data set in section VI.

Lists of conclusions and recommendations derived from this research project are given in section VII. A listing of the Microsoft BASIC source code for the MLIBLAST family of programs can be obtained from the second author at the Structural Development Branch of MSFC.

II. SOFTWARE USER GUIDE

The software developed for this project was written in Microsoft QuickBASIC for DOS. Approximately 0.5 MB of hard disk space, an EGA or VGA graphics card and monitor, and an Intel 80286, 80386, or 80486 CPU is required to run the software. A math coprocessor is desirable, but not required. The software is provided on two 5.25-in, 360K computer disks. A listing of the contents of the computer disks follows:

DISK 1

DATABASE.BAS – source code for the data base creation program (ASCII).

DATABASE.EXE – compiled version of the data base creation program.

DBASEDEL.BAS – source code for the data base record deletion program (ASCII).

DBASEDEL.EXE – compiled version of the data base record deletion program.

DBASEOUT.BAS – source code for the data base viewing program (ASCII).

DBASEOUT.EXE – compiled version of the data base viewing program.

INVRMETH.BAS – source code for the inverse *R* method damage prediction program (ASCII).

INVRMETH.EXE – compiled version of the inverse *R* method damage prediction program.

MATERIAL.DAT – a typical data base file of material properties which is used by the INVRMETH program (ASCII).

MLI.DAT – a typical data base file of experimental results (ASCII).

MLIBLAST.BAS – source code for the main program that runs the other programs (ASCII).

MLIBLAST.EXE – compiled version of the math program.

DISK 2

NONDIMEN.BAS – source code for the nondimensional function damage prediction program (ASCII).

NONDIMEN.EXE – compiled version of the nondimensional function damage prediction program (ASCII).

POLYMETH.BAS – source code for the polynomial function damage prediction program (ASCII).

POLYMETH.EXE – compiled version of the polynomial function damage prediction program.

The software is installed by first creating a subdirectory on the hard disk and then copying all of the files from the two computer disks supplied into that subdirectory. If disk space is a problem, the source code files (*filename*.BAS) need not be copied. The program is started by typing MLIBLAST and following the prompts. More details on the program prompts are given below, but first the data base files MATERIAL.DAT and MLI.DAT will be discussed.

The MATERIAL.DAT that is provided on the program disk is an example of a typical materials data file. Any valid DOS name can be used for this file. Thus, the user may have several of this type of data file in a directory for different purposes. A file of this nature is required while running the inverse *R* program. The materials data file is an ASCII file that can be created and modified using any standard text editor. The format of the file is as follows:

material property 1 name string
material property 2 name string
.
.
.
material property M name string

➤ LISTING OF NAMES OF MATERIAL PROPERTIES TO BE MODELED (MAXIMUM OF 10) (25 CHARACTERS MAX)

{
material 1 name string
material property 1 for material 1
material property 2 for material 1
.
.
.
material property M for material 1
}

➤ TYPICAL DATA RECORD

.
.
.

➤ ANY NUMBER OF DATA RECORDS MAY BE USED

A material data file provided on the computer disk is called MATERIAL.DAT and is reproduced below:

```
Density (lb/in^3)
Elastic Mod. (lb/in^2)
Ultimate Strgth (lb/in^2)
Sp. Heat (BTU/(lb-deg R))
Melting Temp (deg R)
{
1100
 9.780E-2
 1.000E7
 1.600E4
 2.140E-1
 1.680E3
}
{
2219-T87
 1.030E-1
 1.050E7
 6.300E4
 2.050E-1
 1.680E3
}
{
6061-T6
 9.800E-2
 9.900E6
 4.200E4
 2.100E-1
 1.680E3
}
```

The MATERIAL.DAT file listed above is set up to model the material properties: density, elastic modulus, ultimate strength, specific heat, and melting temperature. Other physical properties can be used to a maximum of 10. The units do not have to be included in the material property name string. MATERIAL.DAT contains three records of material data for materials: 1100, 2219-T87, and 6061-T6. The material names are treated as string variables and thus can be any combination of numbers and letters. Any number of records of material data may be included. The order of the material properties must be the same in every record and must be ordered as the material property name strings are listed. For instance, referring to file MATERIAL.DAT, the specific heat of material 2219-T87 is 2.050E-1.

The purpose of the material properties data base file is to provide an efficient, yet very flexible scheme for inputting material property data into the inverse *R* method computer program. The user can easily change the material properties to be modeled without disturbing the data base file of experimental results. If the materials used for the projectile, bumper, and pressure wall do not vary in the data base, then the contents of the material properties data base file will have no effect on the damage predicted by the inverse *R* method program. The polynomial function method program assumes that the material properties do not vary in the data base. The nondimensional function method program assumes that the material properties of the projectile and pressure wall do not vary in the data base and inputs material properties associated with the bumper directly.

The other data base file required for running the programs of MLIBLAST is associated with the experimental data. This file can be created (and enlarged) by running the data base maintenance programs from inside MLIBLAST, or it can be created using any standard text editor since it is an ASCII file. This file can be given any valid DOS file name. Currently, up to 100 data records can be placed in this file. The format for this file is as follows:

{
Test Number String
Test Agency String (SOURCE OF DATA)
Test Date String
Bumper Material String (SAME FORMAT AS IN MATERIAL DATABASE FILE)
Bumper Thickness
Bumper Stand-Off
Pressure Wall Material (SAME FORMAT AS IN MATERIAL DATABASE FILE)
Pressure Wall Thickness
Projectile Material (SAME FORMAT AS IN MATERIAL DATABASE FILE)
Projectile Diameter
Impact Angle
Projectile Velocity
Bumper Hole Maximum Diameter (Major Axis) Dimension
Bumper Hole Minimum Diameter (Minor Axis) Dimension
MLI Mean Hole Diameter
MLI Mass Loss
Pressure Wall Hole Maximum Diameter (Major Axis) Dimension
Pressure Wall Hole Minimum Diameter (Minor Axis) Dimension
}

.
. ➤ AS MANY AS 99 MORE DATA RECORDS
.

MLI.DAT is an example of an experimental data base file. This file is provided on the computer disks. It contains information on the specimens recently used for thermal testing in the Sunspot Thermal Vacuum Chamber of MSFC. To help understand the format information given above, the first record of MLI.DAT is presented below for comparison:

{
1012
MSFC
05/08/90
6061-T6
.08
4
2219-T87
.125
1100
.313
0
6.72
.729
.729
2.2
.938
.6
.15
}

An overview of the menu choices available to the user of MLIBLAST will now be discussed. The program is started by typing MLIBLAST. The user is then provided with three options:

1. Add data to, remove data from, view data, or create a new experimental results data base file. Selecting this option will cause data base maintenance family of programs (DATABASE.EXE, DBASEDEL.EXE, DBASEOUT) to run.

2. Make a prediction. This option involves running one of the three prediction programs: INVRMETH, NONDIMEN, or POLYMETH.

3. Quit MLIBLAST.

The steps associated with running each of the programs will now be considered.

Menu Picks Associated With the Data Base Family of Programs:

1. Add Data to the Data Base (This executes program DATABASE.EXE)

Step 1 – Enter the name of an experimental results data base file. Any valid DOS name can be used. If this file already exists, then the new data records will be appended to the end of it. MLI.DAT is an example of an experimental results data file. This file was provided on the computer disks.

Step 2 – Enter the appropriate data at the prompts. Press ENTER after the data have been typed in. If you make a mistake, then press the F10 function key and then the ENTER key to redo the data input.

Step 3 – You will be prompted as to whether to write your previously entered data record information to your data base file. This provides another way of not saving a data record with errors. You will also be prompted as to whether to enter another data record. A response of *n* will cause you to exit from the data base program. *Note* – the data base file created is an ASCII file which can be edited with a standard text editor. Additional data records can be added to the experimental data base file using the text editor (instead of program DATABASE) if so desired.

2. Delete Data to the Data Base (This executes program DBASEDEL.EXE)

Here the user enters the experimental results data file name, and the test ID and data source of the data record to be removed.

3. Inquire About Data in the Data Base (This executes program DBASEOUT.EXE)

Here the user enters the file name of the experimental results data file to be viewed, and then presses the space bar to page through the data records.

4. Return to Main Menu

This menu choice will return the user to the main menu of MLIBLAST.

Program INVRMETH (See section III for more details on program INVRMETH)

Step 1 – Input the names of the experimental data base file and the material data base file. The program will then read these files and present a summary of their contents on two computer screens. These summary screens are intended to help the user determine if the contents of the data base file are appropriate for the desired prediction.

Step 2 – Select the quantity for which a prediction is to be made. This program is currently designed to make predictions for bumper hole maximum and minimum hole dimensions, MLI average hole diameter, MLI mass loss, and pressure wall maximum and minimum hole dimensions.

Step 3 – Input the impact parameters (such as projectile diameter) associated with the desired prediction. Default values are provided in square brackets for all inputs here except for impact angle. A default value is selected by simply pressing ENTER. The magnitude of the input impact parameter relative to the data base average is indicated in round brackets. For instance, if the projectile velocity for the prediction is twice that of the average projectile velocity in the experimental data base file, the number 2 would appear in round brackets. Ideally, prediction parameter values should be close to the data base average if reliable predictions are to be made. The round bracket numbers are intended to help the user assess the reliability of the prediction.

Step 4 – Review the results of the prediction. Here, the value for the prediction is given, and the location of the prediction point along the prediction vector (see section III) is indicated. Information on the polynomial fit through the 10 interpolation points (see section III) is also provided. The user can also review the results of the prediction graphically. Here, the variation of the function to be predicted along the prediction vector is illustrated to assist the user in assessing the reliability of the prediction. If the function being predicted varies in an erratic fashion along the prediction vector, the prediction may be unreliable.

Program POLYMETH (See section IV for more details on program POLYMETH)

Step 1 – A warning screen is displayed indicating that the program only models the parameters: bumper thickness, bumper standoff, pressure wall thickness, projectile diameter, projectile velocity, and impact angle. All other system parameters are assumed to be essentially constant in the experimental results data base file.

Step 2 – Input experimental results data base file name. No material data file name is requested since it is assumed that material types will not vary in the data base. The program will then read in the contents of the experimental results data base file and display a summary of this data on the screen so that the user may assess its suitability with respect to the required predictions.

Step 3 – Select the desired prediction such as MLI hole diameter.

Step 4 – Input the impact parameters (such as bumper thickness) associated with the prediction.

Step 5 – The program then attempts to fit a linear polynomial through subsets of the data as described in section IV.

Program NONDIMEN (See section V for more details on program NONDIMEN)

Step 1 – Input experimental data base file name. No material data base file name is required because it is assumed that material types will not vary in the data base.

Step 2 – Input bumper elastic modulus (equal to 70E3 MPa for aluminum) and input the mass density of the bumper (equal to 2,710 kg/m^3 for aluminum). After these values have been input, information summarizing the contents of the experimental data base file will be shown on the screen.

Step 3 – Parameters for the nonlinear function coefficient optimizer are input. The purpose of these parameters and recommended magnitudes are displayed on the computer screen.

Step 4 – At this time, an iterative procedure is invoked to adjust the prediction function coefficients such that the coefficient of determination (R^2) is maximized. During this process, the R^2 values are printed on the screen so that the user can assess the suitability of the functional form of prediction equations for fitting the experimental data. Functions that fit the experimental data well will have R^2 values that approach unity.

Step 5 – On completion of the optimization process, the function coefficients and R^2 values are displayed on the screen to further assist the user in assessing the goodness of fit between the functions and the experimental data.

Step 6 – Input prediction parameters (such as bumper thickness) and make predictions.

In the next three sections, more details on the prediction schemes are presented. In section VI, the three prediction schemes are compared using an experimental data set associated with impact specimens that were recently tested in the Sunspot Thermal Vacuum Chamber of MSFC.

III. THE INVERSE *R* PREDICTION TECHNIQUE

The usual procedure for making predictions from experimental data is to assume some form for the equation relating the independent variables to the dependent variable. A function of this nature is described in section V of this report. The equation typically contains empirical coefficients, the values of which are determined from a fit to the experimental data.[4–9] The method of least squares (maximizing the coefficient of determination, R^2) is an example of a popular technique for obtaining the coefficients from the experimental data. The final result is a closed-form equation for making predictions.

This approach has been found to work very well for many engineering applications, however there are some disadvantages. A suitable form for the prediction equation must be developed. This is often difficult. Incorporating additional independent variables in an existing equation can pose problems. Usually, a well-defined procedure for taking into account new experimental data is not put in place. Generally, a single set of empirical coefficients are used to make predictions over a fairly wide range of values of the independent variables. Thus, the best data in a data base for making a prediction with a particular set of independent variables may not be used to best advantage. Also, it is usually difficult to assess the accuracy of a particular prediction.

In this section, a new method (called inverse *R* method) for making empirical predictions based on experimental data is discussed. The method uses a very general form of prediction equation that can be applied in the same manner to all problems. Thus, the user is not required to develop a suitable form for the prediction equation, and additional independent variables can be easily incorporated. The new method is designed to work off a data base that can be continuously updated as new experimental data becomes available. The method automatically takes advantage of the most appropriate data in the data base for a given set of independent variables. The method provides diagnostics for assessing the accuracy of the prediction.

The new technique consists of four main steps which will now be described.

Step 1. Normalize the Independent Variables

In general, the independent variables will vary greatly in magnitude. In hypervelocity impact work, dimensions can be of order 10 and velocities of order 10^6. The new technique requires that all variables be of the same order of magnitude. This was accomplished by scaling the independent variables such that their mean value was equal to unity. Other scaling methods could perhaps be used to improve the accuracy of this technique. For instance, the variables could be scaled such that the predicted values of points in the data base more closely match the measured values. This scaling technique was not tested. The dependent variables need not be scaled.

This technique works off a data base that can and should be kept updated with the latest experimental data. Thus, the scaling factors will change as time progresses and the size of the data base increases.

Step 2. Select a Series of Points in the Data Domain for Interpolation

Two general requirements for prediction schemes are: the method should be capable of smoothing the data to (hopefully) cancel out the random scatter typically present in experimental measurements, and the technique should allow for making reliable predictions outside the domain of the measured data. Here, these requirements are satisfied by using the data to make 10 interpolations from within the domain of the data, which are then used for predicting the dependent variable at some point of interest. The 10 "interpolation" points should provide for sufficient smoothing of the data and also capture the trend characteristics of the data for extrapolation purposes, if an extrapolation is required. The number of interpolation points to use was selected on the basis of trial and error. Note, in some cases extrapolation can produce misleading results regardless of the extrapolation technique used.

Figure 2 provides an illustration of how the interpolation points are selected for a hypothetical case with two independent variables. An identical approach is used for the case of an arbitrary number of independent variables. In figure 2, the independent variables are in the plane of the page, and the dependent variable takes the form of a surface out of the plane of the page.

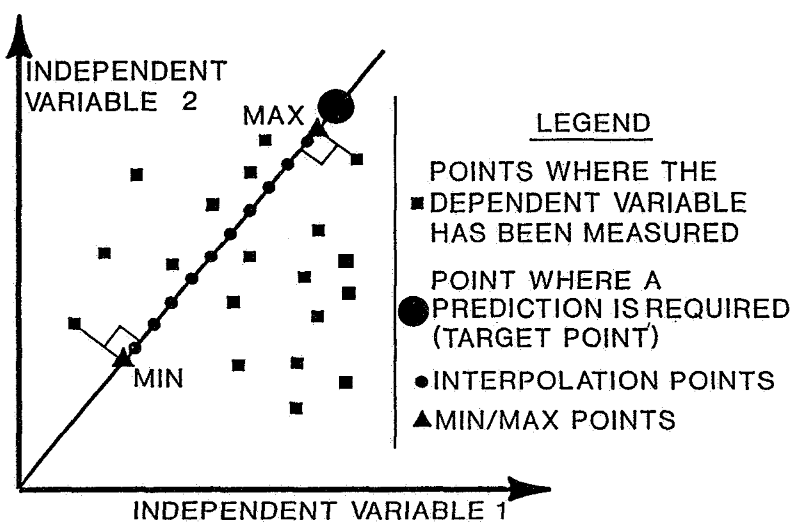

Figure 2. Technique for selecting interpolation point locations for the case of two independent variables.

First, a prediction "vector" is drawn from the origin through the point in the domain where a prediction of the dependent variable is required, which is called the "target" point. Then the "min" and "max" points (fig. 2) are located on the prediction vector by considering the intersection points of perpendiculars from the data points to the prediction vector. The closest intersection point to the origin defines the minimum point, and that of the farthest, the maximum point. Ten equally spaced points (interpolation points) on the prediction vector between the minimum and maximum point are then used for the next step in the prediction process. If the target point lies between the minimum and maximum points, an interpolation is required, otherwise an extrapolation is required.

Step 3. Estimate Values of the Dependent Variable at Interpolation Points

Next, values for the dependent variable must be estimated at the 10 interpolation points. This is done as indicated in the following equation:

$$D = \frac{\sum_{i=1}^{M} \frac{D_i}{R_i^{N-1}}}{\sum_{i=1}^{M} \frac{1}{R_i^{N-1}}} . \tag{3.1}$$

The distances, R_i, are determined by the usual formula for determining the "distance" between two points in an N dimensional space:

$$R_i^2 = \sum_{j=1}^{N} \left(x_{j,i} - x_{j,\mathrm{INT}}\right)^2 , \tag{3.2}$$

where $x_{j,i}$ and $x_{j,\mathrm{INT}}$ are the jth coordinates (bumper thickness and so on) of the data point and the point to be predicted, respectively. The need for scaling the independent variables is evident from considering the form of equation (3.2).

The form of equation (3.1) will now be considered. It is assumed that if all measured data points are the same "distance" R from an interpolation point then all the measured data should be given equal weight. This situation is illustrated for the case of two independent variables ($N = 2$) in figure 3. This can be interpreted as saying that each data point has some "characteristic length of influence," S, that subtends an angle $\theta = S/R = S/R^{N-1}$ as indicated in figure 3. The θ can be taken as the weighting factor. For the constant R case shown in figure 3, all data points would be given the same weight. Figure 4 illustrates the case for which the data points are considered to be equally valid (same S), but are located different distances from the interpolation point. Here, the weighting factors will be of the form $\theta_i = S/R_i^{N-1}$, and thus data points closer to the interpolation point will be given a higher weight. The value of the dependent variable at the interpolation point can be estimated from $D = \sum\theta_i D_i/\sum\theta_i$ which leads to equation (3.1) and, hence, this technique is given the name inverse R method. Note that a value for S is not required as it cancels out of the equation.

The three-dimensional (three independent variables) application of this procedure leads to equations identical in form to those used for determining view factors in the field of radiation heat transfer.[10] The method described herein can be interpreted as follows. The measured data points are "radiating" information to the interpolation point. The farther the data point is away, the weaker the "radiation" (lower weight given to the information). In principle, the method can easily be extended to any number of independent variables, N.

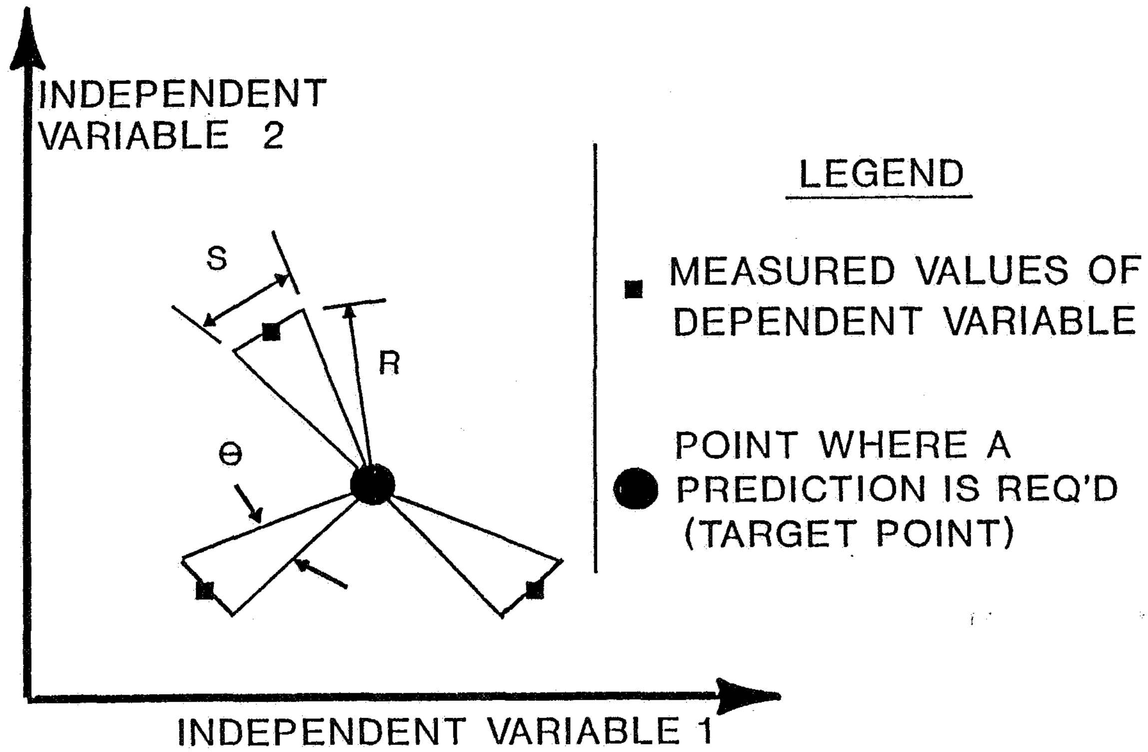

Figure 3. Interpolation scheme for equally spaced data points.

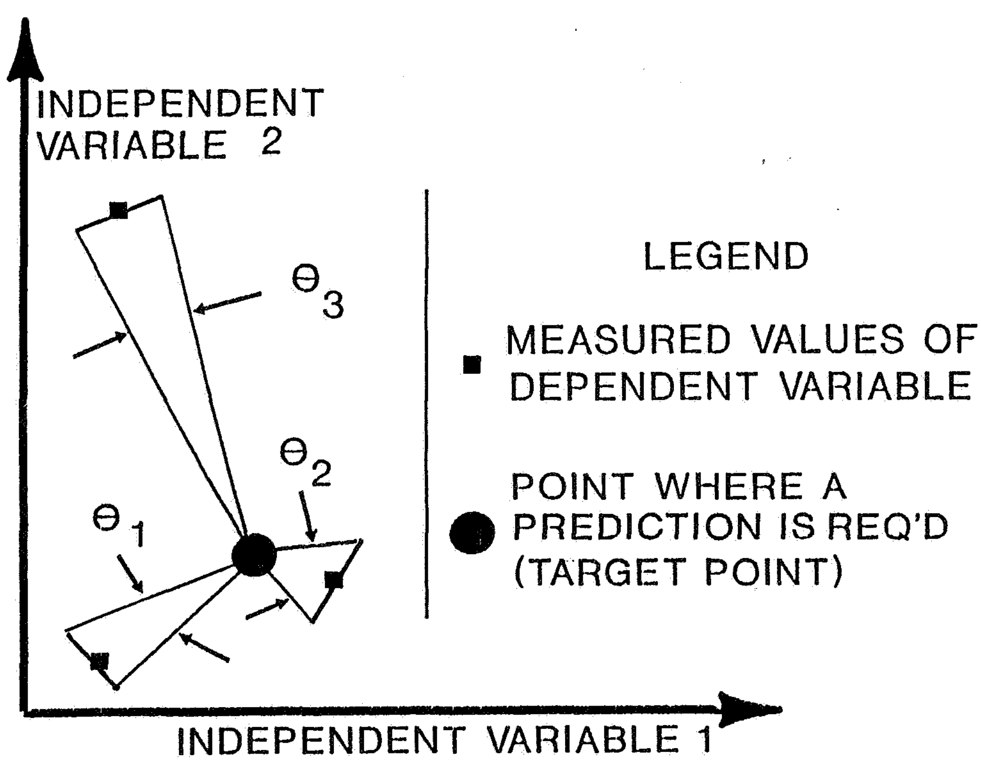

Figure 4. Interpolation scheme for unequally spaced data points.

Step 4. Fit a Polynomial Through the Interpolation Points and Make Prediction

The final step in the process involves fitting a polynomial through the 10 interpolation points and then using the polynomial to make a prediction of the dependent variable at the target point. The polynomial describes how the dependent variable behaves as a function of distance along the prediction vector. By trial and error it was found that a fourth-order polynomial worked well for this application. The polynomial could be used for interpolation or extrapolation depending on the location of the target point. There would, of course, be considerably more uncertainty in the prediction for the case of extrapolation. Errors in the 10 interpolation points tend to get smoothed by the polynomial.

Reliability Diagnostics of the New Interpolation/Extrapolation Technique

The inverse *R* method proposed herein provides diagnostics to help assess the accuracy of the prediction. The computer program provides the user with averages of the independent variables of the data currently in the data base. If the independent variables associated with the target point are close to the data base averages, the user can expect a more reliable result to be produced. The coefficient of determination of the polynomial fit through the 10 interpolation points is presented to the user to assess the scatter in the data. Finally, as shown schematically in figure 5, the 10 interpolation points, the polynomial curve, and the prediction are graphically illustrated on the computer screen to show how the dependent variable behaves as a function of distance along the prediction vector and also indicate the location of the target point along the prediction vector relative to the minimum and maximum points. If the dependent variable oscillates wildly, then unreliable predictions can be expected, particularly for the case of extrapolation. In most cases, target points located approximately halfway between the minimum and maximum points produce the best results.

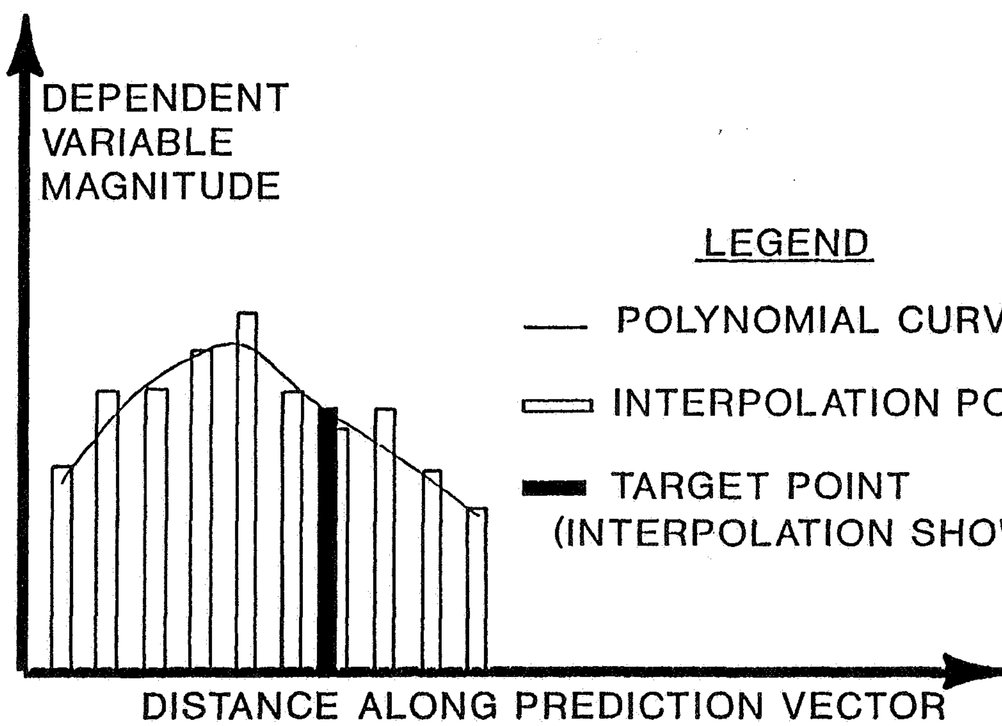

Figure 5. Schematic of prediction reliability diagnostics.

Testing the New Interpolation/Extrapolation Technique

Because of its uniqueness, the inverse *R* method was tested to ensure it would provide reliable predictions. A consistent data base was created using a known function so that the reliability of the prediction could be assessed. The form of the function used was:

$$D_i = \prod_{j=1}^{5} (\text{rn\#}+\text{rn\#}*x_{j,i}+\text{rn\#}*x_{j,i}^2) \quad . \tag{3.3}$$

A set of 15 random numbers, rn#, was required—three for each of the five independent variables used to generate a data set. The random numbers were held constant during the data set creation so that a consistent set of dependent variables were generated. The intent here was to develop an unbiased, sophisticated, and consistent set of data to provide an objective test of the interpolation/extrapolation technique.

The values of the independent variables used were obtained from an actual hypervelocity impact data set (table 1). This data set was selected for two reasons. First, it seemed desirable to use a set of actual engineering data to provide a realistic test of the technique. Secondly, as is discussed below, the inverse *R* method did a poor job of predicting the behavior of some of the experimentally measured dependent variables of table 1. Accordingly, it was of interest to determine if the nature of the data or the prediction technique was at fault for the poor predictions.

Equation (3.3) was used with two sets of random numbers to generate two sets of consistent data. An analysis was done with each set of data as follows. Each record (data point) was temporarily removed from the data base, a prediction was made for the independent variables associated with that record, and then the record was returned to the data base. This was done for all of the 35 records in the data base. Thus, all predictions were made with the actual data point of interest removed from the data base.

A typical set of results is shown in figure 6, where actual data values are plotted against their corresponding predictions. The dashed line in the figure is a linear least-squares fit through the data of the form $y = mx+b$, where y is the prediction, x is the actual function value, and m and b are parameters to be fit. The coefficient of determination of this fit was 0.937. Assuming a functional form of $y = x$ produced a coefficient of determination of 0.934. Similarly, the other consistent data set produced coefficients of determination of 0.961 and 0.959, respectively. Ideally, the prediction, y, should exactly equal the actual value, x, which would result in a coefficient of determination of unity for the line $y = x$.

These results seem to be quite good considering that the dependent variables were reasonably complicated functions of 15 random coefficients with 5 independent variables.

Applying the Inverse *R* Method to Hypervelocity Impact Data

Personnel at MSFC provided the authors with a set of experimentally obtained hypervelocity impact data (table 1). These impact tests were made with the MLI placed directly against the pressure wall as is illustrated in figure 1. The bumper plate was placed approximately

Table 1. Experimental data from hypervelocity impact tests.

Test ID	Bumper Thick. Tb(mm)	Pr. Wall Thick. Tpw(mm)	Proj. Diam. Dp(mm)	Impact Angle θ(deg)	Proj. Vel. V(km/s)	Bump. Maj.Ax. (mm)	Bump. Min.Ax. (mm)	MLI Pen. (cm^2)	MLI Per/Chr (cm^2)	Pr.Wall Maj.Ax. (mm)	Pr.Wall Min.Ax. (mm)
227A	0.81	1.60	6.35	45.00	5.52	15.24	11.68	32.26	51.61	13.46	9.65
227B	0.81	1.60	6.35	45.00	7.12	15.24	10.92	64.52	425.81	25.40	12.70
333	1.02	3.18	4.75	45.00	2.88	10.16	7.62	12.90	32.26	0.00	0.00
334	1.02	3.18	4.75	45.00	3.61	10.16	7.87	8.39	63.23	0.00	0.00
221C	1.02	3.18	4.75	45.00	4.57	11.43	9.14	19.35	51.61	0.00	0.00
221B	1.02	3.18	4.75	45.00	5.89	13.72	10.67	12.90	141.94	0.00	0.00
221A	1.02	3.18	4.75	45.00	6.36	12.19	10.16	12.90	148.39	0.00	0.00
336	1.02	3.18	6.35	45.00	4.47	13.46	10.67	64.52	129.03	14.99	6.35
201B	1.02	3.18	6.35	45.00	5.51	13.46	10.92	64.52	135.48	13.21	11.68
201C	1.02	3.18	6.35	45.00	7.21	13.46	6.35	16.13	161.29	2.54	2.54
203B	1.02	3.18	7.62	65.00	3.67	22.10	11.94	22.58	290.32	0.00	0.00
203A	1.02	3.18	7.62	65.00	6.45	23.88	13.46	29.03	232.26	0.00	0.00
003A	1.02	3.18	7.95	45.00	6.51	19.30	13.72	32.26	129.03	76.20	38.10
338	1.02	3.18	7.95	45.00	6.98	21.34	14.48	83.87	58.06	25.40	17.78
337	1.02	3.18	7.95	45.00	7.00	19.56	13.21	64.52	90.32	27.94	12.70
203F	1.02	3.18	8.89	65.00	3.04	24.89	12.45	13.55	270.97	0.00	0.00
339	1.02	3.18	9.53	45.00	6.49	21.08	17.53	129.03	258.06	50.80	38.10
218B	1.02	4.78	8.89	45.00	6.40	20.32	15.24	51.61	483.87	18.29	15.49
218C	1.02	4.78	8.89	45.00	6.76	21.34	14.99	70.97	270.97	30.73	10.16
230B	1.60	3.18	4.75	45.00	3.23	11.94	9.14	3.87	6.45	0.00	0.00
230A	1.60	3.18	4.75	45.00	4.41	12.19	9.91	6.45	48.39	0.00	0.00
301	1.60	3.18	6.35	45.00	2.95	13.72	10.92	4.26	118.32	0.00	0.00
205A	1.60	3.18	6.35	45.00	4.11	15.49	12.19	11.61	116.13	5.08	5.08
205B	1.60	3.18	6.35	45.00	4.59	16.51	12.45	24.52	335.48	5.08	5.08
205C	1.60	3.18	6.35	45.00	5.30	15.24	12.70	16.13	83.87	7.62	7.62
209B	1.60	3.18	6.35	65.00	6.40	22.10	13.21	5.16	193.55	0.00	0.00
209D	1.60	3.18	6.35	65.00	7.40	19.56	14.48	19.35	206.45	0.00	0.00
207A	1.60	3.18	7.62	65.00	5.86	22.35	14.99	11.61	329.03	4.06	4.06
207C	1.60	3.18	7.62	65.00	7.08	25.91	16.26	103.23	174.19	0.00	0.00
002B	1.60	3.18	7.95	45.00	6.39	20.57	15.75	129.03	77.42	5.59	5.59
211B	1.60	3.18	8.89	45.00	5.85	21.84	17.27	77.42	122.58	27.94	12.70
210B	1.60	3.18	8.89	65.00	5.70	28.70	16.76	41.94	96.77	3.18	3.18
210D	1.60	3.18	8.89	65.00	6.80	35.56	17.27	45.16	212.90	5.84	5.84
303B	1.60	4.06	7.95	45.00	4.34	18.03	14.48	32.90	362.26	0.00	0.00
303	1.60	4.06	7.95	45.00	4.59	18.54	14.73	17.03	166.84	0.00	0.00

100 mm in front of the pressure wall plate. For this series of data, the pressure wall was unstressed. As listed in table 1, the dependent variables measured included the major and minor axis dimensions of the bumper hole, the area of the hole clean through the MLI called the penetration area, the area of MLI outside the penetration area obviously damaged by the impact called the perforated/charred area, and the major and minor axis dimensions of the pressure wall hole. Some comments will now be made on the characteristics of these dependent variables.

The bumper plate hole typically takes the form of a single, well-defined, relatively smooth, elliptical hole. The greater the impact angle, the more elliptical the hole. It is not surprising that the bumper plate hole data are the most consistent of all the data given the relatively simple nature of the damage.

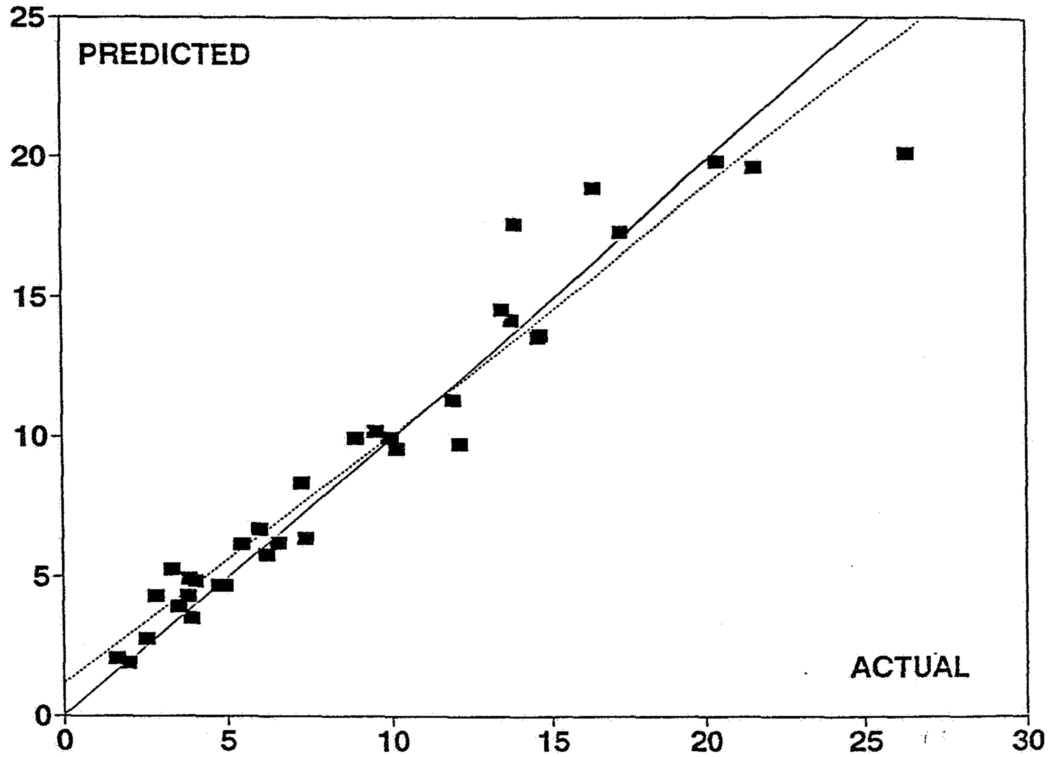

Figure 6. Plot of actual versus predicted values using consistent data.

The remainder of the dependent variables are much more affected by characteristics of the fragmentation/vaporization process of the projectile than the bumper hole is. Launch loads typically cause the soft aluminum projectile to deform into a variety of nonspherical shapes. This effect, and the inevitable presence of a random assortment of microscopic flaws in the projectile and bumper, can cause large variations in the nature of the particles (from both the projectile and the bumper) that leave the back face of the bumper after the bumper-projectile impact. Thus, similar testing conditions can produce significantly different damage to the MLI and the pressure wall.

There is a great deal of inconsistency in the MLI data. In addition to the random processes discussed previously, the inconsistency could be partly due to the difficulty in visually measuring the areas of damage (penetration and perforated/charred) because of the rough, irregular shapes of these areas.

Damage to the pressure wall typically consists of a large number of craters of various sizes, and possibly some penetrations. The craters and penetrations are typically distributed over a relatively large area as can be seen in the photographs of reference 4. The data in table 1 give the dimensions of the largest penetration in the pressure wall, which would essentially depend on the largest fragment that results from the bumper-projectile impact. As has been discussed, apparently identical test conditions could produce a large variation in the size of the largest fragment and, hence, the size of the penetration. This leads to scatter in the pressure wall data.

The procedure described previously that was used to test the inverse *R* technique with the consistent data was also used with the experimental data of table 1. Each record (data point) was temporarily removed from the data base, a prediction made for the independent variables associated with that data point, and then the data point was returned to the data base. The predicted versus actual data are shown in figures 7 through 12. Also drawn on these figures are

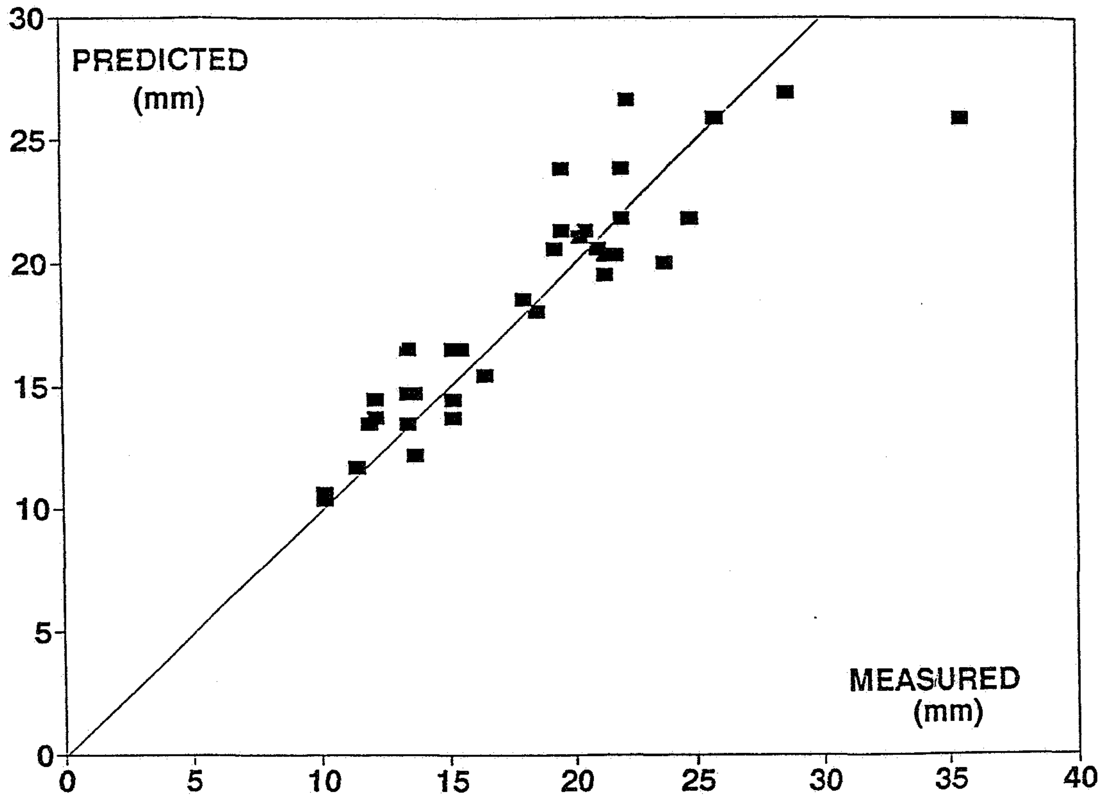

Figure 7. Plot of measured versus predicted data for the major axis of the bumper plate hole.

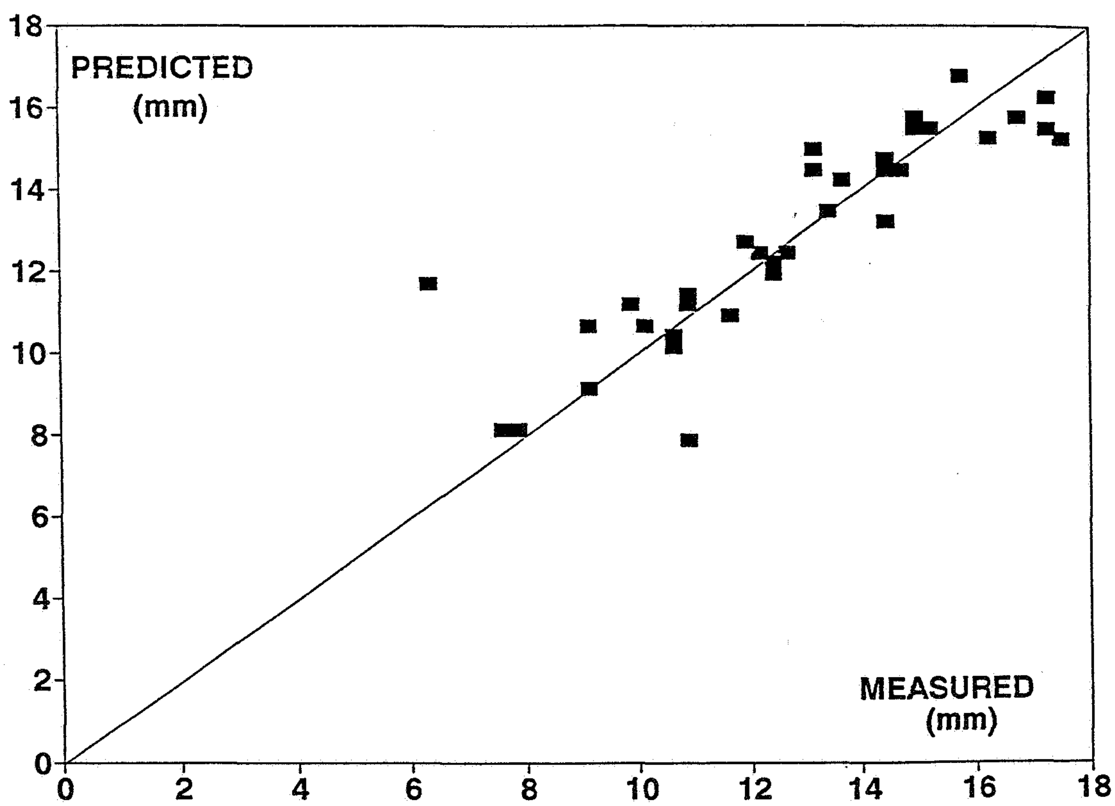

Figure 8. Plot of measured versus predicted data for the minor axis of the bumper plate hole.

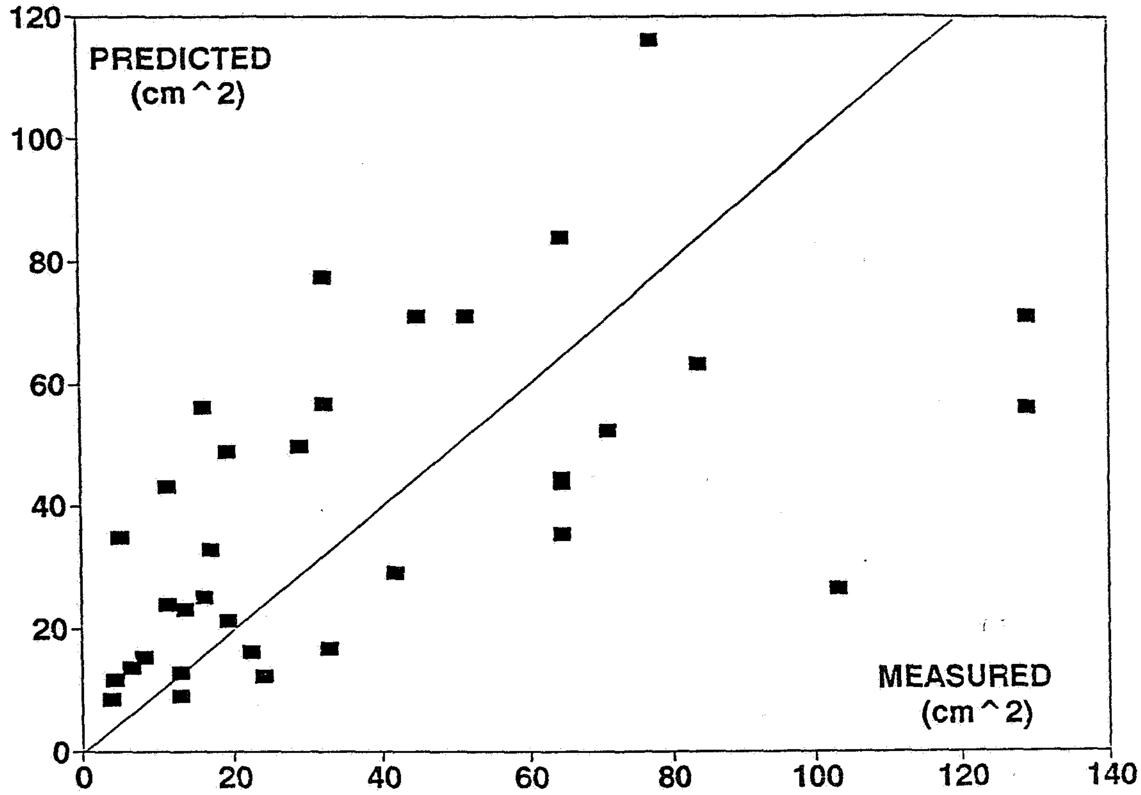

Figure 9. Plot of measured versus predicted data for the MLI penetration area.

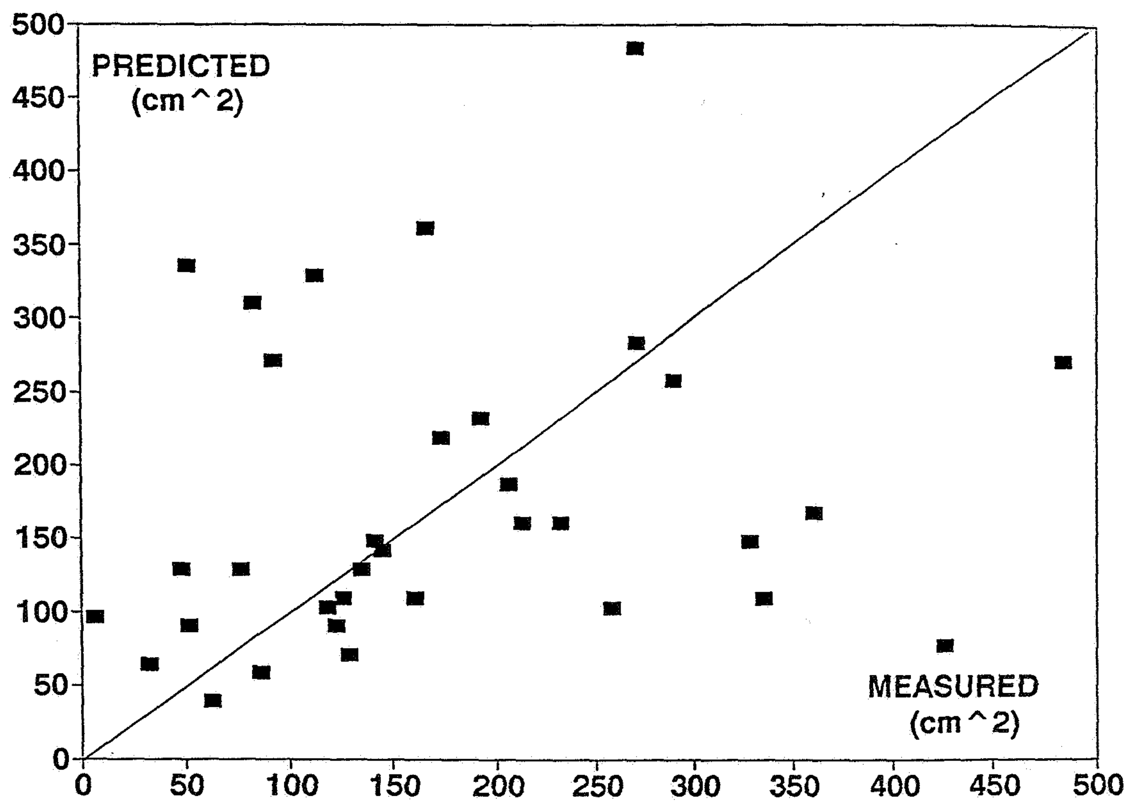

Figure 10. Plot of measured versus predicted data for the MLI perforated/charred area.

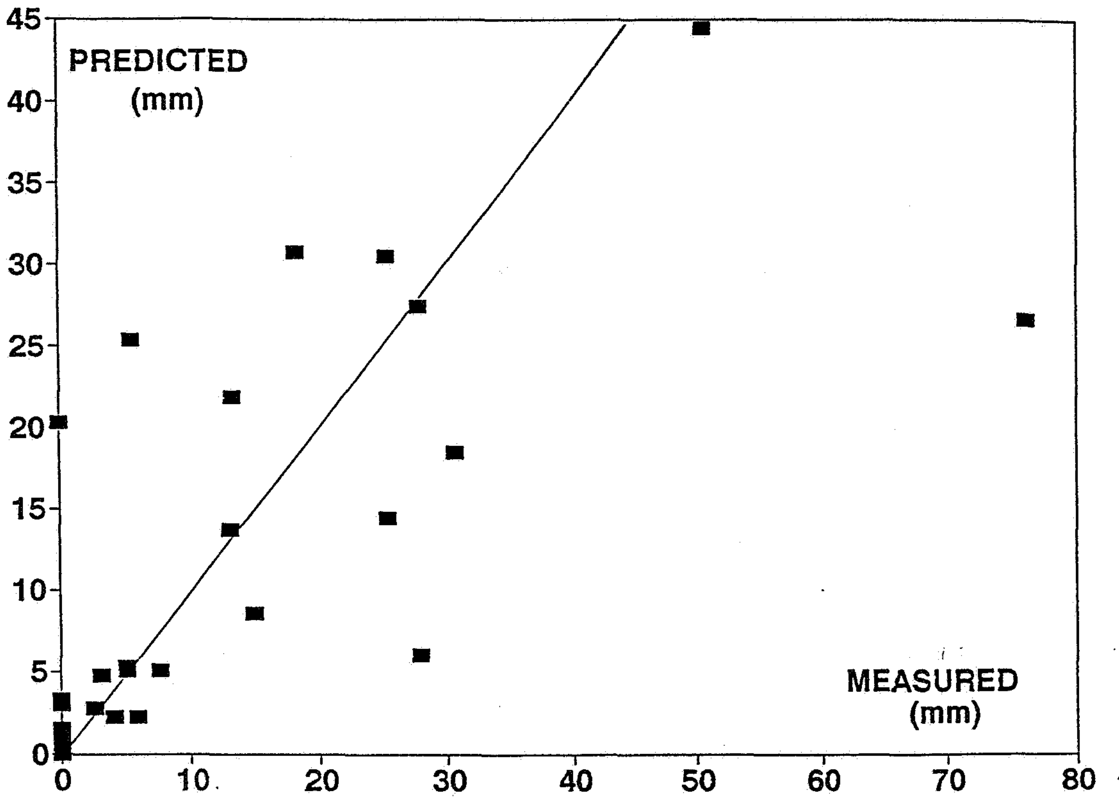

Figure 11. Plot of measured versus predicted data for the major axis of the pressure wall hole.

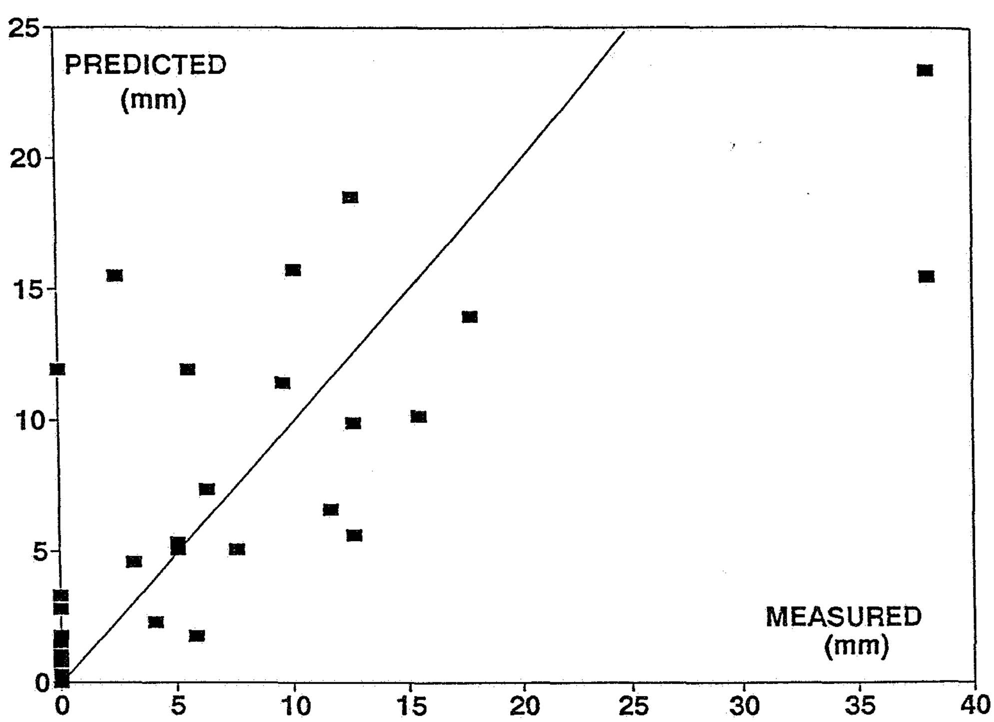

Figure 12. Plot of measured versus predicted data for the minor axis of the pressure wall hole.

solid lines indicating the ideal case of "predicted" = "measured." The coefficients of of determination associated with these predictions are given in table 2. As can be seen from table 2, the predictions for the bumper plate are acceptable. The predictions for the pressure wall are marginal, although figures 11 and 12 are somewhat pessimistic looking since a large number of good predictions were made for data located near the origin of the plots (no penetration case). The predictions of MLI damage are poor for penetration area and terrible for perforated/charred area.

Table 2. Coefficients of determination for predictions.

	Coefficients of Determination (y = prediction, x = measured)	
Data Set	Line of Form y = mx +b	Line of Form y=x
Bumper Major Axis	0.815	0.811
Bumper Minor Axis	0.774	0.773
MLI Penetration Area	0.322	0.289
MLI Perforated/Charred Area	0.042	-0.445
Pressure Wall Major Axis	0.541	0.538
Pressure Wall Minor Axis	0.575	0.566

Since the inverse R technique produced acceptable results for both the consistent test functions of equation (3.3) and the bumper plate data of table 1, the poor predictions of MLI and pressure wall damage are probably due to the scatter in the data produced by such effects as the distortion of the projectile during launch and the apparently random assortment of microscopic flaws in the projectile and the bumper. The inverse R interpolation/extrapolation technique appears to be a useful tool for engineering design work.

IV. THE POLYNOMIAL FUNCTION PREDICTION TECHNIQUE

In this section, the polynomial function prediction technique is described. This method is based on the concepts associated with the FEM. In FEM, relatively low-order polynomials are used to interpolate the functions of interest (such as displacements, temperatures, and velocities) over a small portion of domain where the function is active (called an element). The coefficients of the polynomial are derived from known values of the function of interest at points called nodes on the boundary of the element. For this application, the nodal values of the functions of interest (bumper hole size and so forth) were measured experimentally and are thus known quantities. This technique involves selecting a sufficient number of experimental data (node) points and then determining the coefficients of the polynomial from this data.

During the course of this project, a more sophisticated polynomial interpolation approach was attempted using the isoparametric function mapping technique of FEM. This approach in its current state was not found to be suitable for engineering trade study purposes. The interested reader can consult reference 3 for more details on this approach.

Ideally, the nodes "closest" to the prediction point in impact parameter space should be used to evaluate the polynomial coefficients and thus make a prediction. However, the set of closest nodes may not form linearly independent sets of data, making it impossible to solve for the polynomial coefficients. Thus, remoter nodes must be considered in an attempt to find a linearly independent set of data. The technique used for selecting remoter nodes is discussed below.

In general, the impact parameters will vary greatly in magnitude. In hypervelocity impact work, dimensions can be of order 10 and velocities of order 10^6. This polynomial function approach requires a reasonable scheme for determining "distances" between data points in impact parameter space. This is accomplished in the program by scaling the impact parameters (bumper thicknesses and so on) such that their mean value is equal to unity. Of course, the dependent variables, such as bumper hole size, need not be scaled. Having scaled the independent variables, the usual formula for determining the distance, R_i, between two points (experimental data point and the prediction or interpolation point) in a multidimensional space can be used:

$$R_i^2 = \sum_{j=1}^{N} \left(x_{j,i} - x_{j,\mathrm{INT}}\right)^2 , \tag{4.1}$$

where $x_{j,i}$ and $x_{j,\mathrm{INT}}$ are the jth coordinates (bumper thickness and so on) of the data point and the point to be predicted, respectively. The need for scaling the independent variables is evident from considering the form of equation (4.1).

The form of the polynomial will now be considered. FEM theory dictates that a "complete" polynomial should produce the best results.[11] Here one has six independent variables (bumper thickness and so forth), $x_{j,i}$ (j = 1 to 6), associated with the ith experimental data point to consider. It was decided to use $\Delta x_{j,i}$ ($= x_{j,i} - x_{j,\mathrm{INT}}$) values in the polynomial equation to simplify the calculations. The lowest order complete polynomial for this case is:

$$D_i = C_1 + C_2 * \Delta x_{1,i} + C_3 * \Delta x_{2,i} + C_4 * \Delta x_{3,i} + C_5 * \Delta x_{4,i} + C_6 * \Delta x_{5,i} + C_7 * \Delta x_{6,i} \ . \tag{4.2}$$

Seven linearly independent data points, D_i, are required to determine the seven polynomial coefficients, C_i. Equation (4.2) allows for linear variation in damage along each coordinate axis in the design space. Obviously, allowing for a quadratic variation in the damage would provide a much better fit to the data. Unfortunately, a "complete" quadratic function with six variables would require too many linearly independent experimental data points to be of practical use.

Coefficient C_1 is the prediction of the damage at the point in the design space where the prediction is required, since this is the value of the polynomial (equation (4.2)) when all $\Delta x_{j,i}$ are set equal to zero. If one or more of the prediction parameters, such as bumper thickness, does not vary in the experimental data base file then program POLYMETH will sense this and automatically take that variable or variables out of equation (4.2). If one impact parameter does not vary, only six polynomial coefficients need be determined, and thus only six linearly independent data points are required.

The method used to select the linearly independent set of data points from the data base for determination of the function coefficients, C_i, of equation (4.2) will now be discussed. For illustration purposes, assume that three independent variables are active and, thus, four linearly independent data points are required to fit coefficients C_1 through C_4. First, the four closest data points are selected and tested for linear independence. If they are linearly independent, then the coefficients can be determined and the prediction made. If the four closest data points are not linearly independent, then groups of four data points (the closest data point plus three others) are selected from the closest five data points and tested for linear independence. The first linearly independent set of data points found is used for coefficient determination. If a set of suitable data points is not found, then sets of four data points are selected from the closest six data points and so on.

The number of ways to chose r items from n items, $C(n,r)$, is given by the following equation:

$$C(n,r) = \frac{n!}{(n-r)!r!} \ . \tag{4.3}$$

From equation 4.3, there are 20 ways to choose 3 items from 6 items. Thus, as shown in table 3, 20 sets of data would have to be tested for linear independence when selecting four point data sets (the closest plus three other data points) from the closest seven data points. Note in table 3 that the closest data sets are tested first and data point 1 is always used.

Table 3. Scheme for selecting four data point sets from the closest seven nodes for damage function coefficient determination.

Order In Which Data Sets Are Tested For Linear Independence	Data Points Selected To Form Set Of Four (Ordered From Closest To Prediction Point To Farthest)						
	1	2	3	4	5	6	7
1	1	2	3	4			
2	1	2	3		4		
3	1	2	3			4	
4	1	2	3				4
5	1	2		3	4		
6	1	2		3		4	
7	1	2		3			4
8	1	2			3	4	
9	1	2			3		4
10	1	2				3	4
11	1		2	3	4		
12	1		2	3		4	
13	1		2	3			4
14	1		2		3	4	
15	1		2		3		4
16	1		2			3	4
17	1			2	3	4	
18	1			2	3		4
19	1			2		3	4
20	1				2	3	4

V. THE NONDIMENSIONAL PARAMETER PREDICTION TECHNIQUE

In many applications it has been found that empirical functions are best represented in terms of nondimensional parameters. Reynolds number is an example of a nondimensional parameter that has found widespread use in empirical equations of fluid mechanics. Program NONDIMEN uses a series of empirical functions based on nondimensional parameters of the form given in reference 12:

Bumper Hole Minimum Diameter:

$$\frac{D_{\mathrm{MIN}}}{D_p} = C_1\left(\frac{V}{V_s}\right)^{C_2}\left(\frac{T_b}{D_p}\right)^{C_3}(\cos\phi)^{C_4} + C_5 \ . \tag{5.1}$$

Bumper Hole Maximum Diameter:

$$\frac{D_{\mathrm{MAX}}}{D_p} = C_6\left(\frac{V}{V_s}\right)^{C_7}\left(\frac{T_b}{D_p}\right)^{C_8}(\cos\phi)^{C_9} + C_{10} \ . \tag{5.2}$$

MLI Hole Diameter:

$$\frac{D_{\mathrm{MLI}}}{D_p} = C_{11}\left(\frac{V}{V_s}\right)^{C_{12}}\left(\frac{T_b}{D_p}\right)^{C_{13}}\left(\frac{D_s}{D_p}\right)^{C_{14}}(\cos\phi)^{C_{15}} + C_{16} \ . \tag{5.3}$$

Pressure Wall Average Hole Diameter:

$$\frac{D_{pw}}{D_p} = C_{17}\left(\frac{V}{V_s}\right)^{C_{18}}\left(\frac{T_b}{D_p}\right)^{C_{19}}\left(\frac{D_s}{D_p}\right)^{C_{20}}\left(\frac{T_{pw}}{D_p}\right)^{C_{21}}(\cos\phi)^{C_{22}} + C_{23} \ . \tag{5.4}$$

The function coefficients were determined using an optimization routine to adjust the values of the coefficients so as to maximize the coefficient of determination (R^2) of each of the functions. Thus, the nondimensional functions were adjusted to match the experimental results as closely as possible in a least-squares sense. This approach to coefficient evaluation is suitable for any form of prediction function—linear or nonlinear. The nature of the optimization routine will now be described.

The magnitudes of the function coefficients can vary by several orders of magnitude. To avoid numerical problems, it is advisable to work with percentage changes in the function coefficients. This approach also provides a simple way of controlling the amount of change in the function coefficients from one optimization iteration to the next. If the maximum allowable percentage change is too large, the optimizer could thrash back and forth around the optimum design point without ever converging to it. Alternatively, if the maximum allowable percentage change is too small, then it could take an impractical number of iterations to get to the optimum design point, or the optimizer could get "stuck" in a local maximum of the coefficient of determination function before getting to the global maximum.

The maximum allowable percentage change in the nondimensional function coefficient magnitudes is called the "search domain parameter" in MLIBLAST. This is a user-controlled input parameter. A value of 1.0 (equivalent to a 100-percent change) is recommended. The optimizer is designed to reduce the magnitude of the search domain parameter as the optimization process proceeds. The final value will be 1/100 of the initial value. The idea here is to allow large changes in the design variables initially, to quickly get into the vicinity of the global maximum in the design space, and then use finer steps to precisely locate the global maximum. The user is free to change this parameter to attempt to improve optimization efficiency.

The initial values of the function coefficients are set equal to zero. Optimal values of the function coefficients could be positive, negative, or zero.

The method chosen here for search vector selection is based on Powell's method.[13] This is a first order method that does not require the calculation of the gradient vector. Here, Powell's method was modified as follows. Initially, a number of search vectors equal to the number of function coefficients are created. The components of these vectors are random numbers between –1 and +1. The components of each random search vector are then scaled, such that the largest component has a magnitude of unity. These vectors are stored as columns of a "search matrix." Next, the coefficient of determination is evaluated at the current point in the design space and at design points given by +/– the search domain parameters times the first column of the search matrix. If either of the + or – design points has a coefficient of determination greater than that of the current design point, then the design point corresponding to the highest coefficient of determination will become the new design point. Otherwise, the design point does not change. The search vector multiplier (+/– search magnitude parameter or zero) used with the search vector is stored for later use. This procedure is then repeated with the remaining columns of the search matrix.

A new search vector is created after using all of the search vectors in the search matrix. This new vector is created by vectorially adding together all of the search vectors times their search vector multipliers. The new search vector is a vector sum of previous successful search vectors since unsuccessful search vectors have search multipliers of zero. Thus, the new search vector represents (stores) the trend of the optimization process. The new search vector is scaled such that the magnitude of its largest component is unity and then is used to replace the first column of the search matrix. The procedure is repeated, a new search vector is determined, and then used to replace the second column of the search matrix, and so forth until only the last column of the search matrix remains untouched. Then an entirely new search matrix is created using the random number generator, and the process continues.

If at any time in the iterative process a new search vector has a magnitude of zero (implying all current search directions are not beneficial), then a new random search matrix is created immediately. The random number generator uses a seed based on the number of seconds from midnight on the computer's clock. Each successive run of the optimizer will use a different set of search vectors. Currently, the program runs the optimizer three times (each time using different sets of random search vectors) to help ensure that the global maximum of the coefficient of determination has been located in the design space.

The number of search matrices generated is governed by a user input parameter called the "iteration parameter." The number of random search matrices generated is equal to the number of design variables times the iteration parameter. The recommended value for the iteration parameter is 20.

As can be seen from the test runs of table 4, the optimizer produced very consistent coefficients of determination for all four prediction equations (equations (5.1) to (5.4)). It was noted that virtually identical coefficients of determination could be produced by prediction functions having very different coefficient magnitudes as is illustrated in table 5 for equation (5.3) (MLI hole diameter). This is a typical characteristic of nonlinear equations.

After the prediction function coefficients have been determined and displayed on the screen, the user will be prompted for the impact parameters (such as bumper thickness) associated with the desired predictions. Multiple predictions can be made from the same set of prediction coefficients.

Table 4. Prediction function coefficients of determination for several runs of the optimizer.

Prediction Function	Coefficients of Determination (R^2) Run 1	Run 2	Run3	Run 4	Run 5	Average	Std. Dev.
Bumper Hole Minimum Dia.	0.9946	0.9951	0.9960	0.9945	0.9960	0.9952	0.0006
Bumper Hole Maximum Dia.	0.9949	0.9947	0.9956	0.9952	0.9956	0.9952	0.0004
MLI Hole Diameter	0.9809	0.9809	0.9805	0.9815	0.9814	0.9810	0.0004
Pressure Wall Hole Dia.	0.8292	0.8290	0.8242	0.8290	0.7740	0.8171	0.0232

Table 5. MLI hole diameter prediction coefficients for several optimizer runs.

Optimizer Runs	Prediction Function Coefficients C11	C12	C13	C14	C15	C16	R^2
Run 1	2.860	0.463	-0.390	0.061	-0.356	0.854	0.981
Run 2	2.097	0.570	-0.472	0.042	-0.464	2.100	0.981
Run 3	1.769	0.557	-0.513	0.111	-0.430	1.781	0.981
Run 4	2.697	0.699	-0.489	-0.176	-0.615	3.401	0.982
Run 5	2.690	0.829	-0.552	-0.289	-0.767	4.043	0.981

VI. A COMPARISON OF THE ACCURACY OF THE PREDICTION TECHNIQUES

The accuracies of the three prediction techniques discussed in this report were compared with respect to a common impact data set (table 6). This is the same data set that was recently tested for insulation damage in the Sunspot Thermal Vacuum Chamber of MSFC. These data are also provided on the computer disks as experimental data base file MLI.DAT. These specimens had the MLI mounted next to the bumper during impact testing. Reference 12 contains more general details on the impact testing.

The accuracy of each prediction technique was tested by first removing a data record from the experimental data base file, and then using the remaining data to make a prediction for the impact damage associated with the impact parameters of the removed data record. This was repeated for all of the 19 data records of table 6. The results of this accuracy check are shown in tables 7 to 9 for the three prediction techniques. To compare the accuracies of the three prediction techniques, average percentage differences and coefficients of determination (R^2) were calculated for each of the four prediction functions. These are summarized in table 10. Here, average percentage difference is the average magnitude of the difference between the predicted and measured values divided by the average magnitude of the measured values, times 100. Thus, relatively high average percentage differences indicate that the prediction function did a poor job of predicting the damage.

The following observations can be made about table 10:

1. The poorest predictions by far were made for the pressure wall hole diameter.

2. The best predictions were made for the minimum bumper hole diameter.

3. The inverse R and nondimensional functions did an acceptable job for engineering trade study purposes (average percentage differences < 20 percent) for predicting the bumper hole size and the MLI hole diameter.

4. The nondimensional function technique did the best job overall of predicting impact damage.

The nondimensional functions did the best job of predicting the data of table 6. However, different data sets could produce significantly different results. The nondimensional function approach may not work as well if the prediction parameters (such as impact velocity) cover a greater range in the data base. The inverse R method has the advantage of being able to easily incorporate additional impact parameters. The other two prediction techniques are not as flexible. For instance, the inverse R method would be the method of choice for the case where different materials are used for the bumper in the same experimental results data base file.

Table 6. Experimental data from hypervelocity impact tests for prediction method comparisons.

Test ID	Bumper Thick. Tb(mm)	Pr. Wall Thick. Tpw(mm)	Proj. Diam. Dp(mm)	Impact Angle θ(deg)	Proj. Vel. V(km/s)	Bump. Maj.Ax. (mm)	Bump. Min.Ax. (mm)	MLI Hole Dia. (mm)	MLI Mass Loss (grams)	Pr.Wall Maj.Ax. (mm)	Pr.Wall Min.Ax. (mm)
1012	2.03	3.18	7.95	0	6.72	18.52	18.52	55.88	0.94	15.24	3.81
1029	2.03	3.18	6.35	0	4.98	13.06	13.06	50.80	0.50	3.81	1.02
1028	1.60	3.18	6.35	0	6.98	12.95	12.95	48.26	0.83	2.54	2.54
1026	1.60	3.18	6.35	0	5.22	13.26	13.26	50.80	1.20	0.00	0.00
1018	2.03	3.18	6.35	45	6.28	18.34	14.43	48.26	0.87	8.89	8.89
1020	2.03	3.18	6.35	45	6.91	17.60	15.52	48.26	0.85	1.52	1.52
1017	2.03	3.18	6.35	45	6.20	17.93	17.93	53.34	0.88	5.59	5.59
1019	2.03	3.18	6.35	45	6.84	16.79	14.99	48.26	0.81	8.89	8.89
1027	1.60	3.18	6.35	0	7.05	13.18	13.18	48.26	0.48	4.32	4.32
1035	1.60	3.18	6.35	45	6.21	14.33	13.34	50.80	0.98	6.86	5.21
1034	1.60	3.18	6.35	45	5.20	16.54	13.16	48.26	1.02	3.30	3.30
1016	2.03	3.18	4.75	45	6.13	13.59	12.01	38.10	0.33	0.00	0.00
1023	1.60	3.18	4.75	0	4.18	10.11	10.11	27.94	0.34	0.00	0.00
1025	1.60	3.18	4.75	0	4.63	9.60	9.60	30.48	0.44	0.00	0.00
1033	1.60	3.18	4.75	45	6.28	15.04	11.76	35.56	0.53	0.00	0.00
1021	2.03	3.18	4.75	45	5.65	13.16	11.76	25.40	0.42	1.52	1.52
1032	1.60	3.18	4.75	45	4.75	12.12	10.19	25.40	0.11	0.00	0.00
1024	1.60	3.18	4.75	0	3.79	10.97	9.53	17.78	0.15	0.00	0.00
1031	1.60	3.18	6.35	0	6.98	13.69	12.73	38.10	1.05	0.00	0.00

Table 7. Typical prediction results for inverse *R* impact damage function.

Test ID	Bumper Hole Minimum Dia Measured (in)	Calc (in)	ABS DIFF (in)	Bumper Hole Maximum Dia Measured (in)	Calc (in)	ABS DIFF (in)	MLI Hole Diameter Measured (in)	Calc (in)	ABS DIFF (in)	Pressure Wall Hole Diam Measured (in)	Calc (in)	ABS DIFF (in)
1012	0.729	0.512	0.217	0.729	0.512	0.217	2.2	1.801	0.399	0.375	0.153	0.222
1029	0.514	0.505	0.009	0.514	0.505	0.009	2	1.741	0.259	0.095	0.043	0.052
1028	0.51	0.520	0.010	0.51	0.520	0.010	1.9	1.648	0.252	0.1	0.062	0.038
1026	0.522	0.484	0.038	0.522	0.484	0.038	2	1.638	0.362	0	0.071	0.071
1018	0.568	0.738	0.170	0.722	0.650	0.072	1.9	2.170	0.270	0.35	0.229	0.121
1020	0.611	0.599	0.012	0.693	0.865	0.172	1.9	1.926	0.026	0.06	0.382	0.322
1017	0.706	0.575	0.131	0.706	0.610	0.096	2.1	1.934	0.166	0.22	0.378	0.158
1019	0.59	0.624	0.034	0.661	0.749	0.088	1.9	1.932	0.032	0.35	0.030	0.320
1027	0.519	0.515	0.004	0.519	0.515	0.004	1.9	1.699	0.201	0.17	0.050	0.120
1035	0.525	0.553	0.028	0.564	0.739	0.175	2	1.843	0.157	0.238	0.165	0.073
1034	0.518	0.526	0.008	0.651	0.496	0.155	1.9	1.806	0.094	0.13	0.196	0.066
1016	0.473	0.470	0.003	0.535	0.432	0.103	1.5	1.050	0.450	0	0.066	0.066
1023	0.398	0.395	0.003	0.398	0.395	0.003	1.1	0.881	0.219	0	0.000	0.000
1025	0.378	0.399	0.021	0.378	0.399	0.021	1.2	1.077	0.123	0	0.000	0.000
1033	0.463	0.494	0.031	0.592	0.444	0.148	1.4	1.502	0.102	0	0.101	0.101
1021	0.463	0.478	0.015	0.518	0.595	0.077	1	1.508	0.508	0.06	0.010	0.050
1032	0.401	0.499	0.098	0.477	0.641	0.164	1	1.545	0.545	0	0.086	0.086
1024	0.375	0.397	0.022	0.432	0.397	0.035	0.7	1.107	0.407	0	0.000	0.000
1031	0.501	0.512	0.011	0.539	0.512	0.027	1.5	1.900	0.400	0	0.124	0.124
Averages	0.514	0.515		0.561	0.550		1.637	1.616		0.113	0.113	
Ave % Dif			8.87			15.15			15.99			92.69
R Squared			0.1056			0.2915			0.2659			-0.1638

Table 8. Typical prediction results for polynomial impact damage function.

Test ID	Bumper Hole Minimum Dia Measured (in)	Calc (in)	ABS DIFF (in)	Bumper Hole Maximum Dia Measured (in)	Calc (in)	ABS DIFF (in)	MLI Hole Diameter Measured (in)	Calc (in)	ABS DIFF (in)	Pressure Wall Hole Diam Measured (in)	Calc (in)	ABS DIFF (in)
1012	0.729	0.678	0.051	0.729	0.678	0.051	2.2	2.364	0.164	0.375	0.145	0.230
1029	0.514	0.601	0.087	0.514	0.601	0.087	2	1.402	0.598	0.095	0.323	0.228
1028	0.51	0.520	0.010	0.51	0.520	0.010	1.9	1.710	0.190	0.1	0.085	0.015
1026	0.522	0.414	0.108	0.522	0.414	0.108	2	0.000	2.000	0	0.000	0.000
1018	0.568	0.674	0.106	0.722	0.691	0.031	1.9	1.958	0.058	0.35	0.265	0.085
1020	0.611	0.590	0.021	0.693	0.675	0.018	1.9	2.054	0.154	0.06	0.332	0.272
1017	0.706	0.568	0.138	0.706	0.709	0.003	2.1	1.741	0.359	0.22	0.369	0.149
1019	0.59	0.602	0.012	0.661	0.704	0.043	1.9	1.994	0.094	0.35	0.122	0.228
1027	0.519	0.515	0.004	0.519	0.515	0.004	1.9	1.688	0.212	0.17	0.052	0.118
1035	0.525	0.601	0.076	0.564	0.753	0.189	2	1.887	0.113	0.238	0.269	0.031
1034	0.518	0.489	0.029	0.651	0.488	0.163	1.9	1.744	0.156	0.13	0.233	0.103
1016	0.473	0.415	0.058	0.535	0.477	0.058	1.5	0.905	0.595	0	0.122	0.122
1023	0.398	0.391	0.007	0.398	0.391	0.007	1.1	0.948	0.152	0	0.000	0.000
1025	0.378	0.396	0.018	0.378	0.396	0.018	1.2	0.896	0.304	0	0.035	0.035
1033	0.463	0.416	0.048	0.592	0.380	0.212	1.4	1.417	0.017	0	0.098	0.098
1021	0.463	0.456	0.007	0.518	0.499	0.019	1	1.378	0.378	0.06	0.000	0.060
1032	0.401	0.449	0.047	0.477	0.690	0.213	1	0.983	0.017	0	0.000	0.000
1024	0.375	0.394	0.019	0.432	0.394	0.038	0.7	1.174	0.474	0	0.000	0.000
1031	0.501	0.515	0.014	0.539	0.515	0.024	1.5	1.902	0.402	0	0.133	0.133
Averages	0.514	0.510		0.561	0.552		1.637	1.481		0.113	0.136	
Ave % Dif			8.80			12.16			20.70			88.72
R Squared			0.5934			0.3976			0.1357			-0.0599

Table 9. Typical prediction results for nondimensional impact damage function.

Test ID	Bumper Hole Minimum Dia Measured (in)	Calc (in)	ABS DIFF (in)	Bumper Hole Maximum Dia Measured (in)	Calc (in)	ABS DIFF (in)	MLI Hole Diameter Measured (in)	Calc (in)	ABS DIFF (in)	Pressure Wall Hole Diam Measured (in)	Calc (in)	ABS DIFF (in)
1012	0.729	0.6554	0.074	0.729	0.6554	0.074	2.2	2.1953	0.005	0.375	0.2864	0.089
1029	0.514	0.5382	0.024	0.514	0.5382	0.024	2	1.4637	0.536	0.095	0.2043	0.109
1028	0.51	0.5411	0.031	0.51	0.5411	0.031	1.9	1.8347	0.065	0.1	0.0664	0.034
1026	0.522	0.5374	0.015	0.522	0.5374	0.015	2	1.6192	0.381	0	0.1447	0.145
1018	0.568	0.5972	0.029	0.722	0.6789	0.043	1.9	1.7455	0.154	0.35	0.1535	0.197
1020	0.611	0.6134	0.002	0.693	0.6916	0.001	1.9	2.0017	0.102	0.06	0.3431	0.283
1017	0.706	0.5772	0.129	0.706	0.6792	0.027	2.1	1.8669	0.233	0.22	0.2143	0.006
1019	0.59	0.6013	0.011	0.661	0.6901	0.029	1.9	1.9658	0.066	0.35	0.2109	0.139
1027	0.519	0.5381	0.019	0.519	0.5381	0.019	1.9	1.7567	0.143	0.17	0.1657	0.004
1035	0.525	0.5661	0.041	0.564	0.675	0.111	2	2.0183	0.018	0.238	0.1567	0.081
1034	0.518	0.5412	0.023	0.651	0.6217	0.029	1.9	1.8677	0.032	0.13	0.2277	0.098
1016	0.473	0.4913	0.018	0.535	0.5549	0.020	1.5	1.2275	0.273	0	0.0587	0.059
1023	0.398	0.3896	0.008	0.398	0.3896	0.008	1.1	1.0376	0.062	0	0	0.000
1025	0.378	0.4014	0.023	0.378	0.4014	0.023	1.2	1.07	0.130	0	0	0.000
1033	0.463	0.4502	0.013	0.592	0.5082	0.084	1.4	1.3937	0.006	0	0.0117	0.012
1021	0.463	0.4712	0.008	0.518	0.5535	0.035	1	1.266	0.266	0.06	0.0611	0.001
1032	0.401	0.4216	0.021	0.477	0.5068	0.030	1	1.2965	0.297	0	0.0729	0.073
1024	0.375	0.3784	0.003	0.432	0.3784	0.054	0.7	0.5532	0.147	0	0	0.000
1031	0.501	0.5354	0.034	0.539	0.5354	0.004	1.5	1.9659	0.466	0	0.1033	0.103
Averages	0.514	0.518		0.561	0.562		1.637	1.587		0.113	0.131	
Ave % Dif			5.42			6.21			10.88			66.65
R Squared			0.7397			0.7978			0.7105			0.0035

Table 10. Comparison of the accuracy of the prediction techniques.

Method	Bumper Hole Min. Diameter		Bumper Hole Max. Diameter		MLI Hole Diameter		Pressure Wall Ave. Hole Dia.	
	Ave. % Dif	R Squared	Ave. % Dif	R Squared	Ave. % Dif	R Squared	Ave. % Dif	R Squared
Inverse R	8.9	0.16	15.2	0.29	16.0	0.27	92.7	-0.16
Polynomial	8.8	0.59	12.2	0.40	20.7	0.14	88.7	-0.16
Nondimensional	5.4	0.74	6.2	0.80	10.9	0.71	66.7	0.00

VII. CONCLUSIONS AND RECOMMENDATIONS

As a result of this study the following conclusions were reached:

- There is a large amount of scatter in the hypervelocity impact damage data. It is doubtful that very high prediction accuracies can be obtained regardless of the prediction technique used.

- There is not a great deal of data available for any given set of impact conditions (such as the case with MLI against the bumper). Lack of data prevents higher order prediction functions from being used.

- The inverse *R* method is the most flexible prediction scheme. Any number of impact parameters and any size of data base can be treated.

- The nondimensional parameter functions seem to do the best job of predicting impact damage over a relatively restricted range of impact parameters.

Based on this study the following recommendations are made:

- If possible, all three prediction techniques should be evaluated to determine the best possible prediction technique for a given data set.

- The nondimensional parameter scheme should be used to make impact predictions from data sets for which the impact parameters have a relatively small range.

- The inverse *R* prediction technique should be used in applications where there are a large number of impact parameters (different bumper materials in a single data base file for instance) or where the impact parameters vary over a wide range.

- Numerical simulation results (hydrocode) or approximate analytical results for high velocity (10 to 15 km/s) should be placed in the "experimental" results data base file so that realistic predictions for on-orbit impacts can be made with the software. There are, of course, some uncertainties associated with these high velocity predictions.

REFERENCES

1. Taylor, R.A.: "A Space Debris Simulation Facility for Spacecraft Materials Evaluation." SAMPE Quarterly, vol. 18, February 1987, pp. 28–34.

2. Whipple, F.L.: "Meteorites and Space Travel." Astronomical Journal, No. 1161, 1947, p. 131.

3. Wang, P.: "Multivariable Interpolation and Extrapolation Based on the Isoparametric Concept of the Finite Element Method." MS Thesis, Department of Engineering Mechanics, University of Alabama, Tuscaloosa, 1991.

4. Schonberg, W.P., and Taylor, R.A.: "Penetration and Ricochet Phenomena in Oblique Hypervelocity Impact." AIAA Journal, vol. 27, May 1989, pp. 639–646.

5. Coronado, A.R., Gibbins, M.N., Wright, M.A., and Stern, P.H.: "Space Station Integrated Wall Design and Penetration Damage Control." Boeing Aerospace Company, Seattle, WA, D180-30550-1, July 1987.

6. Fraas, A.P.: "Protection of Spacecraft From Meteoroids and Orbital Debris." Oak Ridge National Laboratory, Oak Ridge, TN, ORNL/TM-9904, March 1986.

7. Gehring, J.W.: "Theory of Impact on Thin Targets and Shields and Correlation With Experiment." High-Velocity Impact Phenomena, R. Kinslow (ed.), First edition, Academic Press, New York, 1970, pp. 117–147.

8. Maiden, C.J., Gehring, J.W., and McMillan, A.R.: "Investigation of Fundamental Mechanism of Damage to Thin Targets by Hypervelocity Projectiles." GM Defense Research Laboratories, Santa Barbara, CA, GM-DRL-TR-63-225, September 1963.

9. Bouma, D.D., and Burkitt, W.C.: "Multivariable Analysis of the Mechanics of Penetration of High Speed Particles." Martin Marietta Corporation, NASA CR-664, December 1966.

10. Özisik, M.N.: "Heat Transfer, A Basic Approach." First edition, McGraw-Hill Book Company, New York, 1985, pp. 593–683.

11. Cook, R.D., Malkus, D.S., and Plesha, M.E.: "Concepts and Applications of Finite Element Analysis." Third edition, John Wiley and Sons, New York, 1989, pp. 82–83.

12. Schonberg, W.P., Bean, A.J., and Darzi, K.: "Hypervelocity Impact Physics." University of Alabama in Huntsville, final report, contract No. NAS8-36955/D.O.16, July 1990.

13. Vanderplaats, G.N.: "Numerical Optimization Techniques for Engineering Design: With Applications." McGraw-Hill Book Company, New York, 1984, pp. 84–87.

APPROVAL

EMPIRICAL PREDICTIONS OF HYPERVELOCITY IMPACT DAMAGE TO THE SPACE STATION

By W.K. Rule and K.B. Hayashida

The information in this report has been reviewed for technical content. Review of any information concerning Department of Defense or nuclear energy activities or programs has been made by the MSFC Security Classification Officer. This report, in its entirety, has been determined to be unclassified.

JAMES C. BLAIR
Director, Structures and Dynamics Laboratory

☆ U.S. GOVERNMENT PRINTING OFFICE 1991— 531—081/40127